A Sampling Theorem for a 2D Surface

Deokwoo Lee and Hamid Krim

Department of Electrical and Computer Engineering
North Carolina State University
Raleigh NC 27606, USA
{dlee4,ahk}@ncsu.edu
http://www.vissta.ncsu.edu/

Abstract. The sampling rate for signal reconstruction has been and remains an important and central criterion in numerous applications. We propose, in this paper, a new approach to determining an optimal sampling rate for a 2D-surface reconstruction using the so-called Two-Thirds Power Law. This paper first introduces an algorithm of a 2D surface reconstruction from a 2D image of circular light patterns projected on the surface. Upon defining the Two-Thirds Power Law we show how the extracted spectral information helps define an optimal sampling rate of the surface, reflected in the number of projected circular patterns required for its reconstruction. This result is of interest in a number of applications such as 3D face recognition and development of new efficient 3D cameras. Substantive examples are provided.

Keywords: Sampling rate, Reconstruction, The *Two-Thirds Power Law*, Structured light patterns.

1 Introduction

Acquisition of 3D images using an active light source has garnered a lot of interest, and has recently been an important topic in vision and image processing. The basis of this active 3D imaging technique is in establishing a geometric relationship between a 3D target and the 2D image of structured light patterns projected on it. In the reconstruction, we assume that the position of the camera and of the light source are known. We also assume that the camera satisfies a pinhole model and the projected light patterns are parallel [1]. The deformation of the circular patterns projected on a 3D object provides sufficient information of the latter's geometrical properties, such as 3D coordinates. In [2], [3], [4] and [5], various algorithms were proposed to improve an accuracy of reconstruction results using structured light patterns. Our approach to the reconstruction is based on exploiting the deformed circular patterns projected on a 3D object [12]. Once 3D coordinates are extracted, *the required minimum number of patterns* to be projected for an efficient reconstruction and minimal computational complexity, is considered. This is tantamount to determining the required sampling rate on the surface for its best reconstruction. Akin to determining the *Shannon-Nyquist Sampling Rate* [6] for a 1D signal, our reconstruction of a 3D signal will seek for

A.M. Bruckstein et al. (Eds.): SSVM 2011, LNCS 6667, pp. 556–567, 2012.

the nontrivial maximal frequency component. Although there have been many contributions ([7], [8]) made for developing a sampling theorem, in this paper, we use the *Shannon-Nyquist Sampling Rate* for a surface reconstruction. The surface of interest has at each point of a projected pattern in $\mathbb{R}^3$ two curvatures, and we use the so-called *Two-Thirds Power Law* [11] to establish a relationship (nonlinear) between a tangential velocity of a curve and these curvatures. Using the equation $V = r\omega$, where V is a tangential velocity, r is the distance from the reference point to an arbitrary point, and $\omega = 2\pi f$ is an angular velocity, we may retrieve the maximum spatial frequency component of the patterns lying on the object (directly related to curvature). The minimum number of patterns is subsequently obtained from the maximum frequency component, which we refer to as a '*curveling rate*' in this paper.

In the following section, we describe an algorithm to extract 3D coordinates using the geometry of the problem. In Section 3, we estimate the frequency components using the *Two-Thirds Power Law* and determine a corresponding sampling rate using the *Shannon-Nyquist Sampling Theorem*. We also substantiate our results by way of experiments in Section 4, followed by some concluding remarks.

2 Geometric Recovery of Surface Coordinates

The substance of this part has appeared in [12] and we hence briefly summarize it here for completeness.

2.1 Geometrical Representation

Let $S \subset \mathbb{R}^3$ be a domain of a 3D object of interest, then a point $P_w \in S$ is represented as

$$P_w = \{(x_w, y_w, z_w) \in \mathbb{R}^3\}, \tag{1}$$

where an index w is used to denote real world coordinates. Let $L \subset \mathbb{R}^3$ be a domain of a circular structured light source, with the origin defined as a center of a pattern (or a curve), then a point $P_L \in L$ is represented as (see Fig. 1)

$$P_L = \{(x_{Lij}, y_{Lij}, z_{Lij}) \in \mathbb{R}^3 \mid x_{Lij}^2 + y_{Lij}^2 = R_j^2,\ z_{Lij} = 0\}, \tag{2}$$

with $i = 1, 2, \ldots, M$, $j = 1, 2, \ldots, N$ respectively indexing the points on the patterns, and the patterns themselves. Let $S_3 \subset \mathbb{R}^3$ be the domain of projected circular patterns on a 3D object, then any point $P_3 \in S_3$ is represented as

$$P_3 = \{(x_{wij}, y_{wij}, z_{wij}) \in \mathbb{R}^3\}, \tag{3}$$

After the patterns projected, P_3 and P_w defined in the intersection of S and S_3 are identical, upon projecting the circular light patterns, P_3 and P_w are to coincide as the intersection of S and S_3,

$$P_3 = \{P_w \mid P_w \in S \cap S_3\} \text{ or } P_w = \{P_3 \mid P_3 \in S \cap S_3\}. \tag{4}$$

Let $S_2 \subset \mathbb{R}^2$ be a domain of a 2D image plane of a camera, then any point $P_2 \in S_2$ is represented as

$$P_2 = \{(u_{ij}, v_{ij}) \in \mathbb{R}^2\}. \tag{5}$$

The 3D reconstruction problem consists of establishing a relationship between $P_3 \in S_3$, $P_L \in L$ and $P_2 \in S_2$ (Fig. 1). Let $f : L \to S_3$ be a map of a light

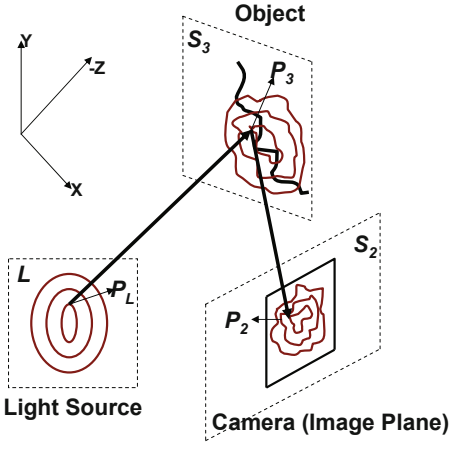

Fig. 1. Geometrical representation of the experimental setup

projection and $g : S_3 \to S_2$ be a map of reflection respectively, then the relevant relationships for surface reconstruction, are

$$f(P_L) = P_3, \quad g(P_3) = P_2. \tag{6}$$

Recall that we assume parallel light projection which preserves (x_{Lij}, y_{Lij}) (i.e. near field projection) and hence the preservation after the pattern projection onto a 3D object so that we have

$$I : (x_{Lij}, y_{Lij}) \to (x_{wij}, y_{wij}), \forall i, j, \tag{7}$$

where I is an identity function. and as discussed previously, under the assumption of parallel projection, (x_{Lij}, y_{Lij}) and (x_{wij}, y_{wij}) obey the following constraints :

$$x_{Lij}^2 + y_{Lij}^2 = R_i^2, \quad x_{wij}^2 + y_{wij}^2 = R_i^2, \tag{8}$$

where i denotes the ith positioned pattern. While coordinates (x_{Lij}, y_{Lij}) are preserved, we note that the depth(z_{wij}) varies and depends on the surface shape. We refer to these variation of depth, z_{wij}, a *deformation factor*. This, in effect, summarizes the reconstruction problem as one of analyzing deformed circular patterns and of depth recovery.

2.2 Mathematical Model

This section details the reconstruction technique of real world 3D coordinates of an object from a planar image of its circularly pattern-lighted surface. The geometrical structure, describing the physical measurement setup, is defined in 3D space and the reference plane is chosen prior to the reconstruction. To solve a reconstruction problem, we opt for two distinct coordinate systems, (X, Z) and (Y, Z) domains(Fig. 2). From Fig. 2, along with associated attributes, we can solve the 3D reconstruction problem. Assuming again that the structured light

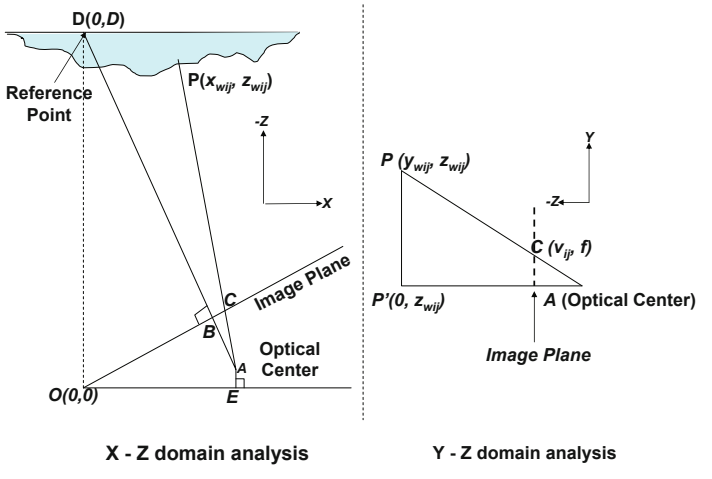

Fig. 2. $(X - Z)$ and $(Y - Z)$ domain analysis

patterns remain parallel, the camera is calibrated to a pinhole model, and its locations together with a chosen reference plane of an object and light source (shown in Fig. 2), we can write the following,

$$\begin{aligned} \overline{AO} = d,\ \overline{AB} = f,\ \overline{BO} = \sqrt{d^2 - f^2} = d_1, \\ d\cos(\angle AOB) = d\cos\theta_2 = \sqrt{d^2 - f^2}, \\ \overline{OC} = |\overrightarrow{OB} + \overrightarrow{BC}|. \end{aligned} \tag{9}$$

Note that the point $C(u_{ij}, v_{ij})$ defined in the 2D image plane, is the result of the reflection of point P, A is the optical center and B is the origin point in the 2D image plane. Since the coordinate system of a 3D object and that of a 2D image plane are different, and upon denoting the $\angle(AOE)$ by θ_1, we transform the domain S_2 to S_3 associated with (X, Z) domain, we can write

$$\begin{aligned} &\theta_1 + \theta_2 = \theta, \\ &A\ :\ (-d\cos\theta_1, d\sin\theta_1), \end{aligned}$$

$$B : (-d_1 \cos\theta, d_1 \sin\theta),$$
$$C : (-d_2 \cos\theta, d_2 \sin\theta), \tag{10}$$

where $\theta_1, \theta_2, \theta, d, d_1$ and d_2 are known calibrated quantities. Using the intersection point A of lines $\overline{PC}$ and $\overline{DB}$ (see Fig. 2), we can write a relationship between x_w and z_w. To completely reconstruct the 3D coordinates (x_w, y_w, z_w), we can show the (Y, Z) domain analysis (Fig. 2). Using the above relationships, we can determine 3D coordinates of the deformed curves on a surface,

$$F(x_{wij}) = z_{wij}, \quad H(x_{wij}) = z_{wij}. \tag{11}$$

In [12], we detailed the above relationships and illustrated the approach.

3 Sampling Rate Determination

Using the 2D images of the projected patterns on a surface, and the development described above, we proceed to the surface reconstruction. Each image consists of all curves resulting of the structured circular light patterns. Upon the recovery of 3D real coordinates, the required minimum number of circular patterns for 3D reconstruction is considered. In this section, we develop the minimum sampling rate, to in turn, specify the necessary number of circular patterns required for reconstruction. Recall that the required minimum number of circular pattern is referred to as a *curveling rate*, and preceding its determination, a maximal frequency component of an object should be retrieved. To estimate the frequencies, we apply the *Two-Thirds Power Law* [10] which unveils a relationship between the motion of a shape/curve and its characteristics. Specifically, the radius of curvature(R) of on an osculating circle around a closed curve, and its tangential velocity(V) satisfy the Eq. (12), where K is a constant depending on duration of the motion [10], and α and β are parameters to be estimated [9]. Note that the parameter β is very close to two thirds (2/3), as has been shown by [13]. Projected circular patterns on a 3D object (Fig. 3) have two tangential vectors. Hence, each 3D point of the surface of interest, has two curvature components (κ_{1ij} and κ_{2ij}), the first derivatives of tangential vectors, T_{1ij} and T_{2ij} with respect to the arc length (see Fig. 4). The two-thirds power law can be written as

$$V = r\omega = K \cdot \left(\frac{R}{1 + \alpha R} \right)^{1-\beta}, \tag{12}$$

where r is a distance between the reference point(i.e. nosetip) and the arbitrary point of the object (Fig. 4). According to Eq. (12), we can acquire two frequency components corresponding to κ_{1ij} and κ_{2ij}, respectively.

$$\omega_{1ij} = 2\pi f_{1ij} = \frac{1}{r_{1ij}} \cdot \left(\frac{R_{1ij}}{1 + \alpha R_{1ij}} \right)^{1-\beta}, \tag{13}$$

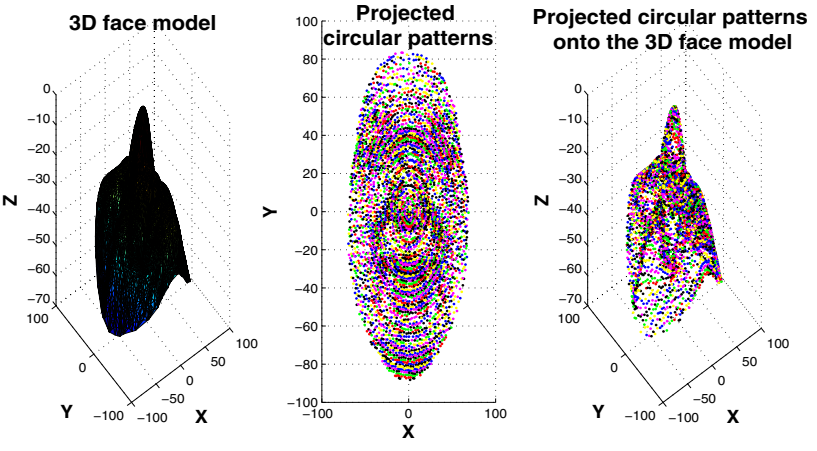

Fig. 3. Simulation of projection of circular patterns, (a). 3D face model, (b). Circular patterns, (c). Overlaying patterns.

$$\omega_{2ij} = 2\pi f_{2ij} = \frac{1}{r_{2ij}} \cdot \left(\frac{R_{2ij}}{1 + \alpha R_{2ij}} \right)^{1-\beta}, \tag{14}$$

$$r_{1ij} = r_{2ij} = r_{ij},\ i = 1, 2, \ldots, M,\ j = 1, 2, \ldots, N, \tag{15}$$

where R_{1ij} and R_{2ij} are $\frac{1}{\kappa_{1ij}}$ and $\frac{1}{\kappa_{2ij}}$, respectively, and M is the number of points of each curve and N is a number of curves(patterns) on the surface. To determine the minimum sampling rate($2 \times \max(f_{ij})$) which is determined by the *Nyquist Rate*, the maximum frequency component, $\max(f_{ij})$ is required, and we define $\max(f_{ij})$ as

$$\max(f_{ij}) = \max[sup(f_{1ij}), sup(f_{2ij})]. \tag{16}$$

Using a relationship between a frequency component, f_{ij} and the corresponding r_{ij}, the maximum frequency is calculated. Prior to measuring the maximum f_{ij}, $sup(f_{1ij})$ and $sup(f_{2ij})$ should be acquired, and each of which satisfies the following,

$$sup(f_{kij}) \leq \frac{1}{2\pi} sup\left(\frac{1}{r_{kij}} \cdot \left(\frac{R_{kij}}{1 + \alpha R_{kij}} \right)^{1-\beta} \right), \quad k = 1, 2. \tag{17}$$

Prior to measurement of curvatures and r_{ij}'s of all the points of the deformed circular patterns, a normalization of data points is carried out. The normalization yields the determination of the intrinsic characteristics of each curve projection on the surface.

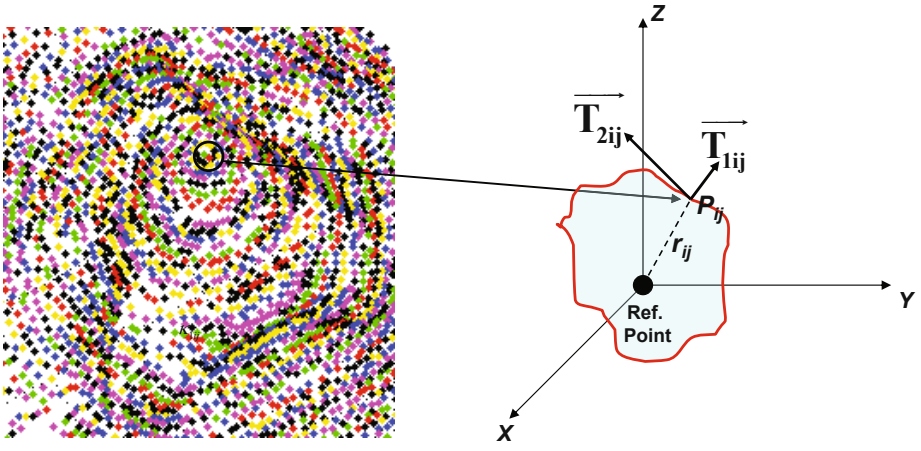

Fig. 4. Two tangential vectors of a point on a 3D object. The first derivative of a tangential vector is a curvature.

4 Experimental Results

To substantiate the measurement of frequency components steps, some simulated examples are shown in this section. Initial number of projected patterns are different from each other and related to the characteristics of objects. The maximum frequency component of the jth curve, $\max[(f_{ij})]_{j=1}^{N}$, measured through all the points of a curve is shown in Fig. 5. From the simulated result in Fig. 5, the maximum frequency component is 0.1501 and the minimum sampling rate is $0.1501 \times 2 = 0.3002$. To substantiate the determination of the above surface sampling rate, we propose some numerical examples. The initial number (N_{ini}) of the projected patterns are determined by the characteristics of the surface. The first (Fig. 6)and the second (Fig. 9) example surfaces consists of 89 and 110 circular patterns, respectively. These numbers correspond to infinite sampling rate in a continuous domain. *Curveling rate*(N_s), the minimum number of patterns defined as

$$N_s = \lceil 2 \times \max[f_{ij}]_{i=1,j=1}^{M,\ N} \times N_{ini} \rceil, \tag{18}$$

and estimated N_{ini}, $\max[f_{ij}]$ and N_s are provided in Table.1. To evaluate the accuracy of a reconstruction, the L_2-norm distance between the original($S_O \subset \mathbb{R}^3$) and the reconstructed surfaces($S_R \subset \mathbb{R}^3$) is computed through all the pixels.

$$d_2(S_O, S_R) = ||S_O - S_R||_2 = \left(\sum_{p_O, p_R \in \mathbb{R}^3} [p_O - p_R]^2 \right)^{1/2}, \tag{19}$$

where $d_2(S_O, S_R)$ is an L_2-norm distance(geometric error), and $p_O \in S_O$ and $p_R \in S_R$ represent 3D Euclidean coordinates of the original and the

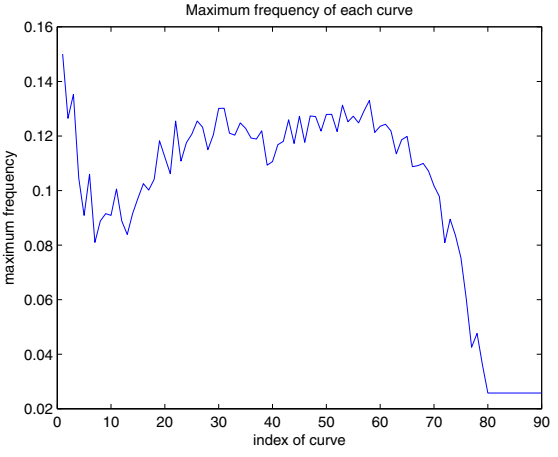

Fig. 5. Maximum frequency components of curves(from the j = 1th to Nth curve) on the 3D face model(Fig. 6). Frequency is defined in a unit space(arc length) and quantities are relative each other. In this example, $\max[f_{ij}]$ is 0.1501 and the sampling rate is 0.3002.

Table 1. Estimated *curveling rate* of two face models

	N_{ini}	$\max[f_{ij}]$	N_s
Face 1	89	0.1501	27
Face 2	110	0.1984	44

reconstructed surfaces, respectively. Simulated examples of S_R and $d_2(S_O, S_R)$ are shown in Fig.s. 7, 8, 10 and 11.

5 Conclusion and Future Works

In this paper we have presented an algorithm to determine the sampling rate of a surface (or defining the minimum number of light patterns to be projected on a surface whose maximal curvatures may be known) subjected to an active light source probing. Such a rate, in turn plays a key role in the efficient representation of a surface and its subsequent reconstruction from these patterns. While our primary application of interest lies in the area of biometrics and face modeling, the two-thirds-based sampling criterion may be exploited in many different settings where surface representation and sampling are of interest (e.g. surface archiving). We have also shown some illustrative examples. Although our sampling rate does not recover the surface perfectly as the *Shannon-Nyquist Sampling Rate* does for 1D signals, the sampling criterion we proposed does not show a considerable information loss to be recognized. In the future, there are

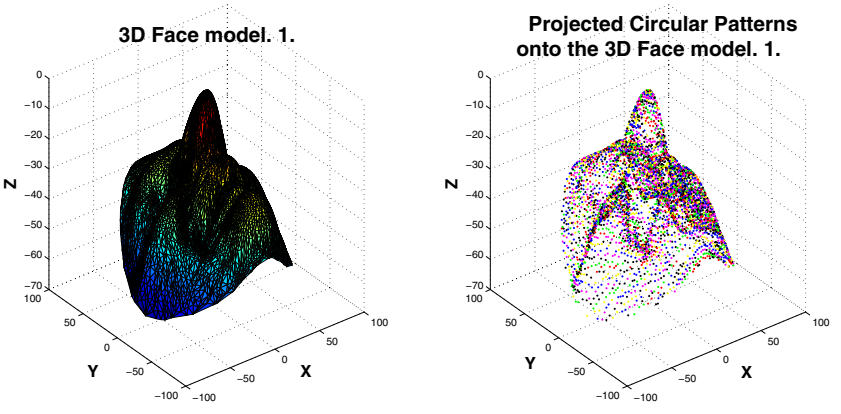

Fig. 6. Original 3D *Face1* model(left), Projected circular patterns onto the 3D face model(right)

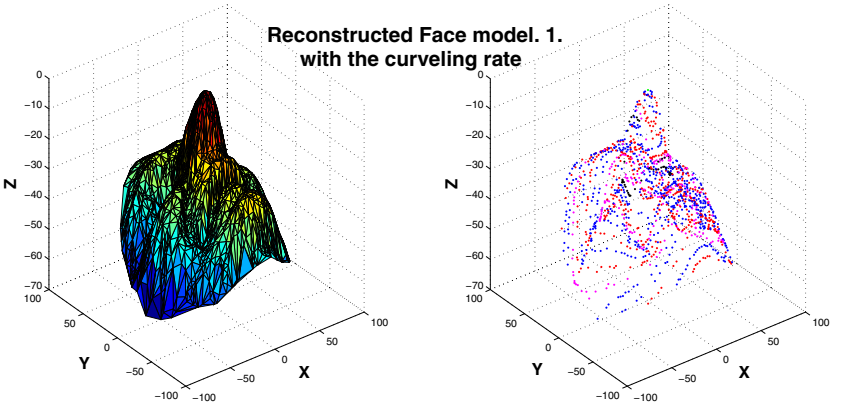

Fig. 7. Reconstructed 3D *Face1* model from the curveling rate 27

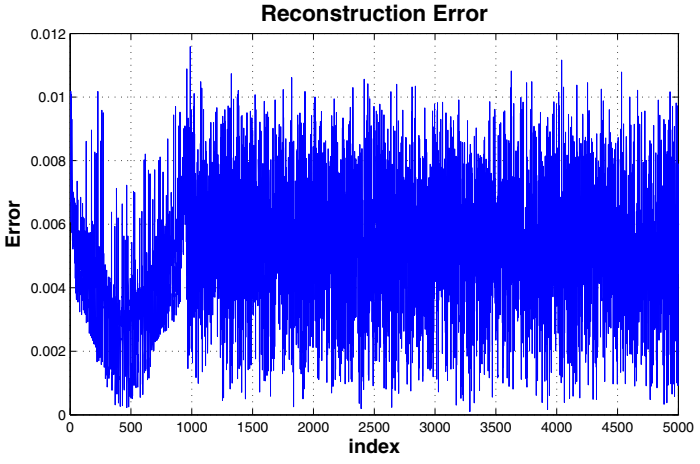

Fig. 8. The L_2-norm distance between the original and the reconstructed *Face1* model (Fig.s 6 and 7)

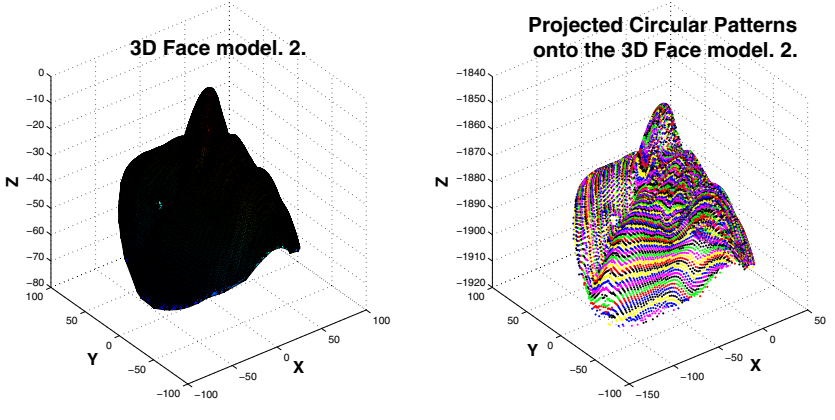

Fig. 9. Original 3D *Face2* model(left), Projected circular patterns onto the 3D face model(right)

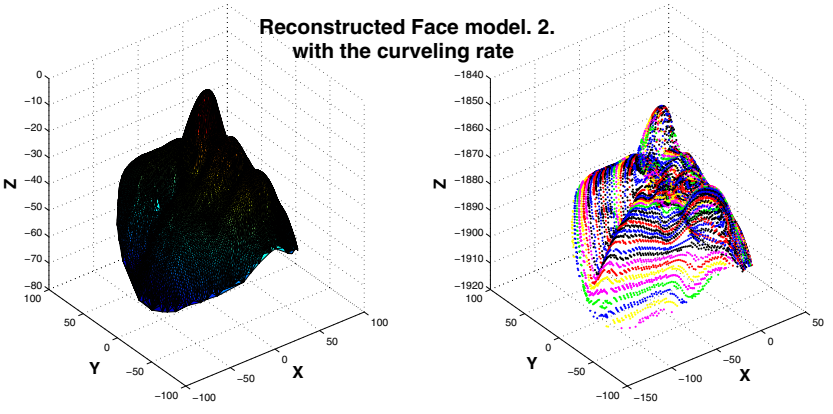

Fig. 10. Reconstructed 3D *Face2* model from the curveling rate 44

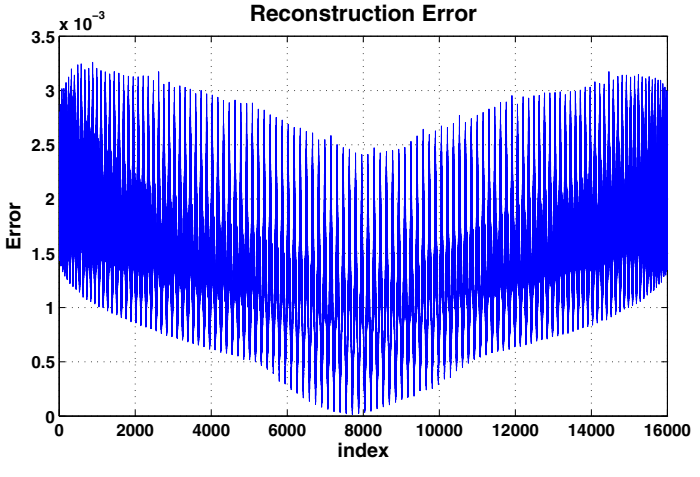

Fig. 11. The L_2-norm distance between the original and the reconstructed *Face2* model (Fig.s 9 and 10)

some technical issues to be considered - quantifying the algorithm efficiency (i.e. computational complexity) and the reconstruction accuracy compared to the previous methods is needed and being in progress.

References

1. Faugeras, O., Luong, Q.-T.: The Geometry of Multiple Images (2001)
2. Wei, Z., Zhou, F., Zhang, G.: 3D coordinates measurement based on structured light sensor. Sensors and Actuators A: Physical 120, 527–535 (2005)
3. Asada, M., Ichikawa, H., Tsuji, S.: Determining of surface properties by projecting a stripe pattern. In: Proc. Int. Conf. on Pattern Recognition, pp. 1162–1164 (1986)
4. Dipanda, A., Woo, S.: Towards a real-time 3D shape reconstruction using a structured light system. Pattern Recognition 38, 1632–1650 (2005)
5. Batlle, J., Mouaddib, E., Salvi, J.: Recent Progress in Coded Structured Light as a Technique to solve the Correspondence Problem: A Survey. Pattern Recognition 31, 963–982 (1998)
6. Papoulis, A.: Signal Analysis. McGraw-Hill, New York (1977)
7. Eldar, Y.C.: Compressed Sensing of Analog Signals in Shift-Invariant Spaces. IEEE Transactions on Signal Processing 57(8) (August 2009)
8. Jerri, A.J.: The Shannon Sampling Theorem - Its Various Extensions and Applications: A Tutorial Review. Proceedings of The IEEE 65(11) (November 1977)
9. Maoz, U., Portugaly, E., Flash, T., Weiss, Y.: Noise and the two-thirds power law
10. de' Sperati, C., Viviani, P.: The Relationship between Curvature and Velocity in Two-Dimensional Smooth Pursuit Eye Movements. The Journal of Neuroscience 17, 3932–3945 (1997)
11. Schaal, S., Sternad, D.: Origins and violations of the 2/3 power law in rhythmic 3D movements. Experimental. Brain Research,, 60–72 (2001)
12. Lee, D., Krim, H.: 3D surface reconstruction using structured circular light patterns. In: Blanc-Talon, J., Bone, D., Philips, W., Popescu, D., Scheunders, P. (eds.) ACIVS 2010, Part I. LNCS, vol. 6474, pp. 279–289. Springer, Heidelberg (2010)
13. Lacquaniti, F., Terzuolo, C., Viviani, P.: The law relating the kinematic and figural aspects of drawing movements. Acta Psychologica, 115–130 (1983)
14. Pollefeys, M., Koch, R., Van Gool, L.: Self-Calibration and Metric Reconstruction Inspite of Varying and Known Intrinsic Camera Parameters. International Journal of Computer Vision, 7–25 (1999)
15. Armangue, X., Salvi, J., Batlle, J.: A Comparative Review Of Camera Calibrating Methods with Accuracy Evaluation. Pattern Recognition 35, 1617–1635 (2000)
16. Sturm, P.: On Focal Length Calibration from Two Views. In: IEEE International Conference on Computer Vision and Pattern Recognition, pp. 145–150 (2001)